Pure & Appl. Chem., Vol. 64, No. 6, pp. 893–902, 1992.
Printed in Great Britain.

S-band electron spin echo spectroscopy

R. B. Clarkson[†‡], D. R. Brown[*], J. B. Cornelius[*], H. C. Crookham[*], W.-J. Shi[*], and R. L. Belford[*‡]

Department of Veterinary Clinical Medicine[†], Department of Chemistry[*], and Illinois EPR Research Center[‡], University of Illinois, Urbana, IL 61801 USA

Abstract

In order to explore the advantages of multi-frequency ESE experiments, we have constructed a pulsed EPR spectrometer operating over a microwave frequency range of 2-4 GHz (S-band). Dramatic enhancement of electron spin echo envelope modulation (ESEEM) depth is observed for weakly coupled nuclei. Well-defined resonance peaks corresponding to nearly pure NQR frequencies are observed for ^{14}N in some nitroaromatic systems, at values of B_o near "exact cancellation" and more distant from the cancellation condition than had been predicted. In the case of nitrogen modulation in a copper(II) complex with large *g* anisotropy, strong orientation selection is achieved at S-band as well as X-band; the S-band spectrum is different and complementary.

INTRODUCTION

Electron spin echo envelope modulation (ESEEM) experiments have proven to be very useful in measuring weak hyperfine interactions in paramagnetic solids. While most ESE experiments have been performed at X-band (9 GHz), instances in which other frequency ranges are advantageous have been noted [1 - 6]. The advantages offered by employing higher frequencies include greater sensitivity, improved orientation selection in disordered anisotropic systems, and the ability to study systems with large zero-field splitting [6]. Frequencies below X-band have been demonstrated to be useful for direct determination of nuclear quadrupole couplings by reducing the nuclear Zeeman interaction enough to approach a cancellation of the nuclear hyperfine coupling by the nuclear Zeeman interaction in one of the electron spin manifolds [7 - 10]. Lower frequencies also will be useful as part of a multi-frequency approach to ESEEM [11]. Just as in cw EPR [12], a multi-frequency approach will allow a more reliable determination of the spin Hamiltonian parameters. For systems where field-dependent terms dominate the nuclear spin Hamiltonian at X-band, a substantial improvement in the observed modulation depth is expected when ESEEM is performed at lower frequency (lower field). Also, lower frequencies should lead to better resolution in the sum peak, thus further improving the ability of ESEEM experiments to observe small structural differences. For such reasons, we constructed a broadband pulsed EPR spectrometer operating between 2 and 4 GHz, the S-band of microwave frequencies. We report here on the design and describe several recent applications of this spectrometer.

EXPERIMENTAL

A. Instrumentation

A block diagram of the S–band ESE spectrometer is shown in Figure 1. The microwave bridge is very similar to a standard EPR bridge. The major differences are the fast PIN diode switches and the high power, pulsed TWT amplifier. The purpose of these components is to create the short, high power microwave pulses needed in the ESEEM experiment. The transistor oscillator (KDI Electronics, model no. CC-A24) serves as the microwave source, tunable from 2 to 4 GHz. The oscillator is followed by an isolator (UTE Microwave, model no. CT-3240-OT) to protect it from reflected microwave power. A -20dB directional coupler (Narda, model no. 4013C-20) diverts a small portion of the power to a frequency meter followed by a -10 dB directional coupler (Narda, model 4013C-10) which diverts power into the reference arm. The remaining power is fed into a PIN diode switch (General Microwave,

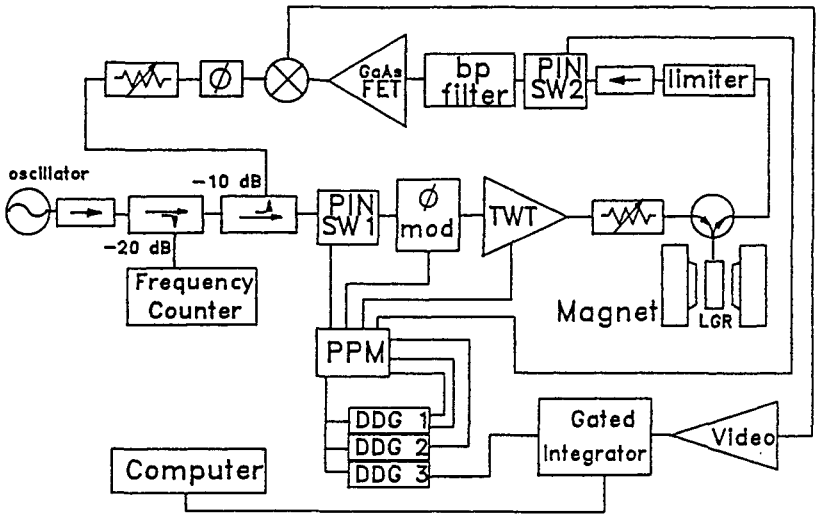

Figure 1. Block diagram of the S-band pulsed EPR spectrometer. [13]

model DM863BH) in order to create short, low power pulses. Next the microwave phase of these pulses can be shifted by 180° by a one-bit digital phase shifter (Vectronics Microwave, model DP613.OHS) and then they are amplified by a 1kW TWT amplifier (Logimetrics, model A710/S). The TWT is driven as near to saturation as possible and the power of the pulses is adjusted by the step attenuator (Weinschel, model AC117A-69-11) which follows the TWT. Now the pulses are ready to be fed through a 3-port circulator (UTE, model CT-3242-0) into a loop-gap [14] or bridged loop-gap [15] resonator structure placed between the poles of an electromagnet and accommodates the sample to be studied. Any power reflected from the resonator is then directed by the circulator into the bridge's detection elements. The power limiter (Miteq, model LIM-2040-20) serves to protect the low noise GaAs FET amplifier (Miteq, model AMF-48-2040-7-L) from the high power pulses. A second PIN diode switch is used to gate off the input to the GaAs FET during the pulses providing added protection for the GaAs FET and keeping the mixer (Watkins-Johnson, model WJ-M1G) out of saturation during the pulses. Since the PIN diode switch is reflective in its off state, it is preceded by an isolator. For some experiments, a 2 to 4 GHz bandpass filter (K&L Microwave, model 3H10-1000/4000-0/0) was placed after the second PIN diode switch to remove RF switching transients produced by the switch. The power and phase of the reference signal can be adjusted by an attenuator (Weinschel, model 910-20-11) and a phase shifter (Narda, model 3752), both continuously variable. The IF output of the mixer is boosted by two video amplifiers (Hewlett-Packard, model 461A and Comlinear, model CLC100). The echo amplitude is averaged by a gated integrator (EG&G PARC, model 162 boxcar averager with two model 166 gated integrators) whose output is then sampled and stored by a computer.

The timing of the ESEEM experiment is controlled by three delay units (Figure 1). Each repetition of the spin echo sequence is initiated by a clock signal from an IBM Data Acquisition and Control (DAC) adapter in an IBM PC. The clock signal triggers 3 Berkeley Nucleonic Corporation model 7030A digital delay generators (DDGs). The DDGs in turn control the pulse widths and the timing of the interval between pulses. The pulse widths are set manually with a knob on the front of each DDG. The DDGs are remotely programmed through a parallel interface on each generator connected to a Quatech PXB-721 parallel I/O card installed in the computer. Pulses produced by the DDGs are fed into the pulse programming module (PPM), which creates the appropriate signals for triggering the PIN switches, the phase modulator and the TWT grid control.

The S-band pulsed spectrometer currently is capable of one-, two-, and three-pulse experiments with (0, π) phase cycling utilizing a one-bit digital phase shifter, although a two-bit shifter is now being installed that will permit (0, $\pi/2$, π, $3\pi/2$) phase sequences. Detailed descriptions of the electronics and software can be found in references [13] and [16].

B. Samples

Perylene cation radicals were formed on the particle surfaces of powdered activated silica-alumina (Houdry M-46 catalyst), by a technique already described [17]. A similar approach, utilizing activated γ-alumina in place of the silica-alumina, was employed for the formation of meta-dinitrobenzene (m-DNB) radical anions.

Solutions of 1,1-diphenyl-2-picrylhydrazyl (DPPH) in toluene were prepared by dissolving the DPPH powder (Aldrich Chemical Co., 95% pure) in appropriate amounts of toluene (normal or d_8, Fischer Scientific, A.C.S. certified). Solutions were placed in 4mm quartz tubes and thoroughly de-gassed by freeze-pump-thaw cycling before flame sealing.

Bis(1-phenyl-1,3-butanedionato)copper(II) (Cu(benzac)$_2$) was prepared by the method of Hon, et. al. [18], except that the final product was recrystallized twice from toluene. Solutions of Cu(benzac)$_2$ with pyridine (Aldrich Chemical Co., 99+%, spectrophotometric grade, gold label) in toluene (Fischer Scientific, A.C.S. certified) were prepared with concentrations of the copper complex set at about 5 mM. The mixed solvent was ca. 33% in pyridine (producing mainly the •2Py adduct) or ca. 5 mM (producing mainly the •Py adduct).

C. Spectroscopy

Both two- and three- pulse (Hahn and stimulated) spin echo sequences were performed on all samples at various S-band frequencies. Temperatures were controlled by means of an APD helium flow cryostat fitted with a locally-constructed Dewar extension (silvered Pyrex) that allowed the loop-gap resonator assembly to be inserted into the thermostatted flowing helium stream. A temperature of ca. 4K was reached with the helium flow rapid enough to force liquid helium over the resonator. At lower flow rates, with gaseous helium bathing the resonator, temperatures over the range from 280K to ca. 8K could be controlled with this arrangement, which allowed for quick sample changing without warming the resonator. For analysis, ESEEM data can be transformed to the frequency domain by means of a cosine Fourier transform algorithm that utilizes the frequency windowing approach of Mims [19]. Simulation of the time domain data often is done by means of a theoretical model implemented in a computer program called NANGSEL. This program (developed by Professor J. B. Cornelius in this laboratory, at Albert Einstein College of Medicine, and at Principia College) employs a powder-average algorithm and provides for the inclusion of anisotropic g- and A-matrices for orientation-selected ESEEM analysis [20].

EXPERIMENTAL RESULTS AND DISCUSSION

A. Enhancement of modulation depth in perylene cation radical spectra

A quantitative estimate of the degree to which shallow modulation from a weakly coupled system at X-band (9 GHz) can be enhanced by going to S-band (2-4 GHz) can be obtained by examining the analytical expression for the 2-pulse modulation function, which can be written for the $S=1/2$, $I=1/2$ case with a spin Hamiltonian of the form, $\hat{\mathcal{H}} = g\beta_e H_0 \hat{S}_z - g_n\beta_n H_0 \hat{I}_z + \hbar A \hat{I}_z\hat{S}_z + \hbar B \hat{I}_x\hat{S}_x$, as shown in equation (1). The depth of the modulation is governed by k, which has been aptly termed the modulation depth parameter. When the nuclear Zeeman interaction is much larger than the hyperfine interaction, $\omega_n \approx \omega_\alpha \approx \omega_\beta$ and

$$\begin{gathered} E_{mod}(\tau) = 1 - 2k\,\sin^2(\tfrac{1}{2}\omega_\alpha\tau)\sin^2(\tfrac{1}{2}\omega_\beta\tau) \\ \text{where } k = \omega_n^2 B^2/\omega_\alpha^2\omega_\beta^2, \quad \omega_n = g_n\beta_n H_0/\hbar \\ \omega_\alpha^2 = [(\tfrac{1}{2}A+\omega_n)^2+(\tfrac{1}{2}B)^2],\ \omega_\beta^2 = [(\tfrac{1}{2}A-\omega_n)^2+(\tfrac{1}{2}B)^2] \end{gathered} \tag{1}$$

$k \approx B^2/\omega_n^2$. Since ω_n is proportional to the applied magnetic field and B is independent of field, $k \propto 1/H_0^2$. Thus, for this system, k is expected to be 9 times as large at 3 GHz (S-band) than at 9 GHz (X-band).

Predictions of enhanced modulation depth at S-band were tested for the perylene radical cation formed on active silica-alumina surfaces. This species has been studied by ENDOR [17,21], and the distant or matrix proton interactions have been identified with solvent and surface hydrogens. Figure 2 shows X- and S-band ESEEM patterns attributed to these matrix protons, after normalization to remove the decay function. At both frequencies, τ values were

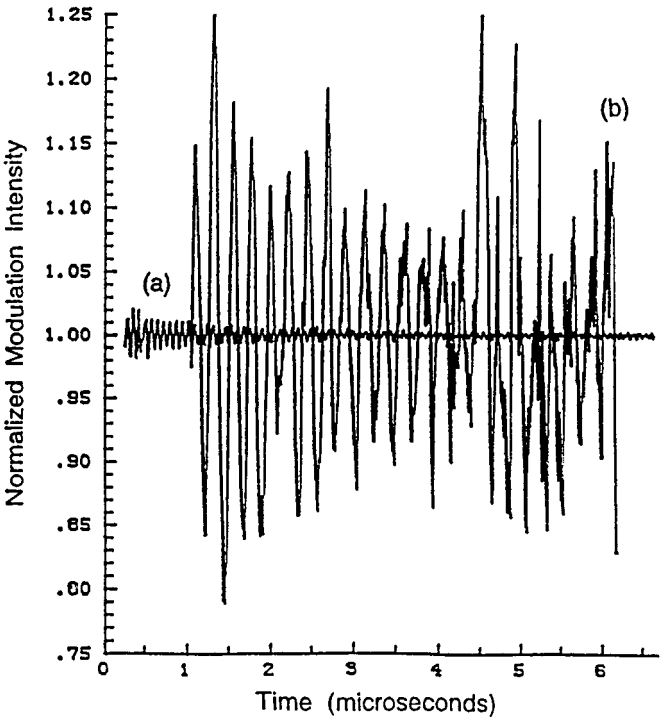

Figure 2.
Normalized echo envelope modulation from perylene(+) radicals after removal of the echo decay function.
(a) X-band ESEEM,
(b) S-band ESEEM.
Spectra taken at 5K. [22].

chosen to maximize proton modulation. A nine-fold enhancement of the modulation depth at S-band over X-band seen in the patterns is agrees with that predicted for a decrease in magnetic field (microwave frequency) by a factor of 1/3. All systems where weakly coupled nuclei are observed by two- or three-pulse echo sequences exhibit similar behavior.

B. Nuclear quadrupole couplings in DPPH

For a quadrupolar nucleus such as ^{14}N ($I = 1$) in systems where the hyperfine coupling to nitrogen is dominated by an isotropic interaction, it sometimes is possible to observe nearly pure nuclear quadrupole resonance (NQR) transition frequencies in the ESEEM. This is an important application of pulsed EPR, for it makes possible the observation of NQR transition frequencies from paramagnetic species in which the enhanced nuclear relaxation due to effects from the paramagnetic electron may prohibit the direct measurement of the NQR spectrum. It also offers a more sensitive spectroscopic approach, thus permitting the study of systems too dilute for conventional NQR studies, such as biological samples. Two studies have considered this NQR contribution to the ESEEM pattern from solid solutions of DPPH, one at X-band [23], and one at X- and C-band (4.6 GHz) [5]. In the latter study, the theory of which they subsequently published in more detail [24], Flanagan and Singel suggest that the observation in ESEEM of narrow linewidth resonances corresponding to nearly pure NQR frequencies occurs when $B_o = A_{iso}/2g_n\beta_n$, where B_o is the applied Zeeman field, and A_{iso} is the isotropic hyperfine coupling. At this equivalence point, "exact cancellation" of the hyperfine and Zeeman fields is envisioned, resulting in an effective field of zero at the nucleus. As in other zero-field resonance experiments, this results in substantial narrowing of surviving resonance lines. Making use of ^{14}N NMR data on DPPH [25], one can use this cancellation condition to predict that the equivalence point ($B_{eff} = 0$) for the ortho and para NO_2 nitrogens in DPPH should occur at a field value where the microwave resonance frequency is in the range 5.0 - 5.9 GHz.

How far from the exact cancellation field will we still expect to see narrow resonances corresponding to nearly pure NQR frequencies? Flanagan and Singel [24] suggest that if Δ is the deviation from exact cancellation, that the NQR frequencies will be observed if $|\tilde{\Delta}| < 4\tilde{K}/3$, where $\tilde{\Delta} = \Delta/\nu_n$, and $\tilde{K} = K/\nu_n$, $K = \frac{1}{4}e^2qQ$. To test this model, we obtained ESEEM from frozen solutions of DPPH in toluene at 3.0 GHz (1078 Gauss), where no NQR frequencies from either ortho or para NO_2 nitrogens should be seen ($\tilde{\Delta} \geq 1.3$, $4\tilde{K}/3 = 1.1$), and at 4.02

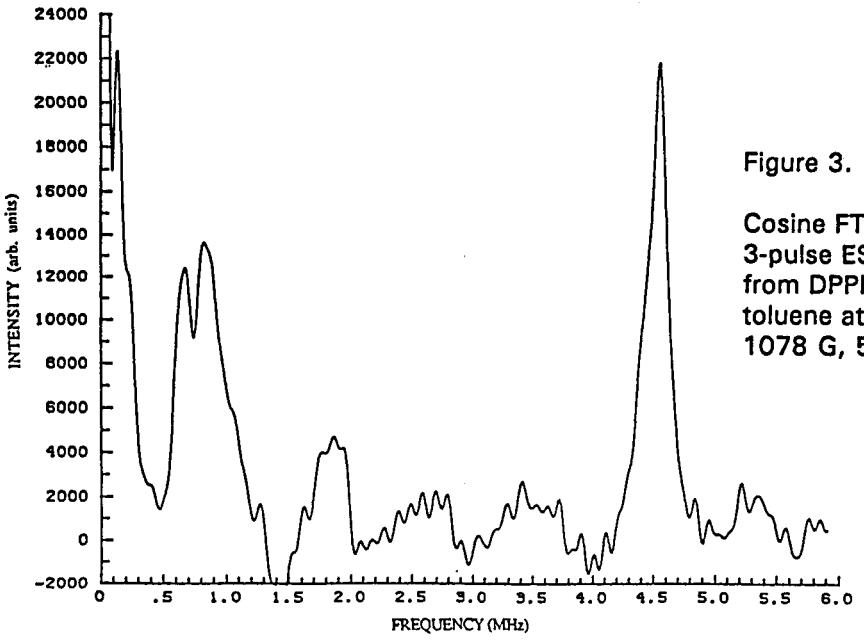

Figure 3.

Cosine FT of 3-pulse ESEEM from DPPH in toluene at 3.0 GHz, 1078 G, 5K.

GHz (1437 Gauss), where sharp transitions from ortho NO_2 and possibly from para NO_2 nitrogens are predicted ($\tilde{\Delta}_{ortho}$ = 0.49, $4\tilde{K}/3$ = 0.84). Figure 3 shows a cosine FT of the ESEEM pattern obtained at 3.0 GHz from a stimulated echo sequence. The sharp pair of frequencies at 0.68 and 0.87 MHz, which are also seen at 4.02 GHz and are insensitive to B_o, are attributed to the ν_- and ν_+ NQR transitions from ortho NO_2 nitrogens. The 1.86 MHz line is assigned to the $\Delta M_I = 2$ transition of ^{14}N, in the nuclear manifold in which exact cancellation does not occur, and shifts with B_o in accord with predictions that its frequency should be approximately $A_{iso} + 2\nu_n$. The resonance at 4.5 MHz is due to matrix protons. Based on this assignment of ν_+, ν_-, the quadrupole parameters for ortho nitrogens in DPPH are calculated to be K = 0.26±0.02 MHz, and η = 0.35±0.02, and $A_{iso}(^{14}N_{ortho})$ = 1.19 MHz. Singel recently reported values of K = 0.28 MHz, η = 0.37 and A_{iso} = 1.12 MHz for this system from C-band measurements [26], at Zeeman field strengths very near that predicted for "exact cancellation". The excellent agreement of our calculated quadrupole parameters and A_{iso} with those of Singel give support to our spectral assignments, and suggest that nearly pure NQR frequencies can be seen in ESEEM patterns at microwave frequencies considerably below the low-field limit of the effect suggested by Flanagan and Singel.

C. $Cu(benzac)_2$–pyridine adducts

Cu(II) β-ketoenolates are prototypical metal complexes which have been widely studied by EPR, UV-VIS, and X-ray crystallography as well as other forms of spectroscopy. For this reason, they provide excellent frames of reference (though not necessarily model compounds) for studies of other metal complexes such as metalloproteins which are not yet well characterized. Since the Cu(II) β-ketoenolates are so well characterized they make ideal test subjects for developing new experimental methods of characterization.

An important aspect of the chemistry of Cu(II) β-ketoenolates is their capacity to act as Lewis acids forming adducts with a variety of Lewis bases such as water, ethanol, and pyridine. Generally these adducts are not amenable to analysis by X-ray crystallography because the adducts are too unstable to be isolated from solution. On the other hand, some structural information can be deduced from the anisotropic spin Hamiltonian parameters obtained from EPR studies of frozen solutions. Unfortunately, the information acquired from such EPR spectra is usually limited to the parameters which determine the electronic Zeeman, copper electron-nuclear hyperfine and copper electric quadrupole terms in the Hamiltonian. A much more detailed structural picture can be pieced together if ligand hyperfine and quadrupole couplings are available but the small spectral splittings associated with such interactions are usually obscured by inhomogeneous line broadening.

Several investigations have been successful in determining ligand spin Hamiltonian parameters applying orientation-selective ENDOR and ESEEM techniques. Kirste and van Willigen have determined hyperfine matrices for the CH and CH_3 protons of bis(acetylacetonato)copper(II) ($Cu(acac)_2$) and several of its adducts with ENDOR and electron-nuclear-nuclear triple resonance [27]. Similarly Henderson, Hurst, and Kreilick have determined the proton hyperfine matrices for polycrystalline samples of $Cu(acac)_2$ with orientation selective ENDOR [28]. More recently, Cornelius and co-workers has examined an adduct of bis(1-phenyl-1,3-butanedionato)copper(II) ($Cu(benzac)_2$) with pyridine by ESEEM at X-band in an effort to determine the nitrogen hyperfine and ^{14}N quadrupole coupling parameters [20,29]. Here we report S-band ESEEM measurements on this system.

Time domain ESEEM spectra were recorded from samples with equimolar concentration of $Cu(benzac)_2$ and pyridine and from samples with a large excess of pyridine (solutions in 33% pyridine, 67% toluene by volume). Samples prepared with d_5-pyridine and d_8-toluene were also examined. Two pulse spectra on the samples prepared with protiated solvents show a small splitting of the proton "sum" peak (the peak located at approximately twice the proton Larmor frequency). This splitting varies considerably with field. In addition to possible orientation selection effects, the sum peak will in general exhibit field sensitivity, since the structure-sensitive frequency of the peak maximum, $\nu_{max} = (\Delta + 2\nu_n)$, where Δ is the frequency shift associated with A_{iso}. Sum peak resolution of small structural differences thus can be enhanced at lower Zeeman fields, where shifts of ν_{max} will be proportionately greater, since the contribution of ν_n is reduced relative to Δ. Figure 4(a) shows a frequency domain representation of the two pulse ESEEM spectrum taken from the parallel (low field) region of the EPR spectrum where the proton sum peak splitting is the largest. In Figure 4(b), the frequency domain spectrum obtained from the perpendicular region reveals that the sum peak splitting in this region is much smaller. The spectra from samples prepared with deuterated solvents show only deep modulation near the free deuterium Larmor frequency.

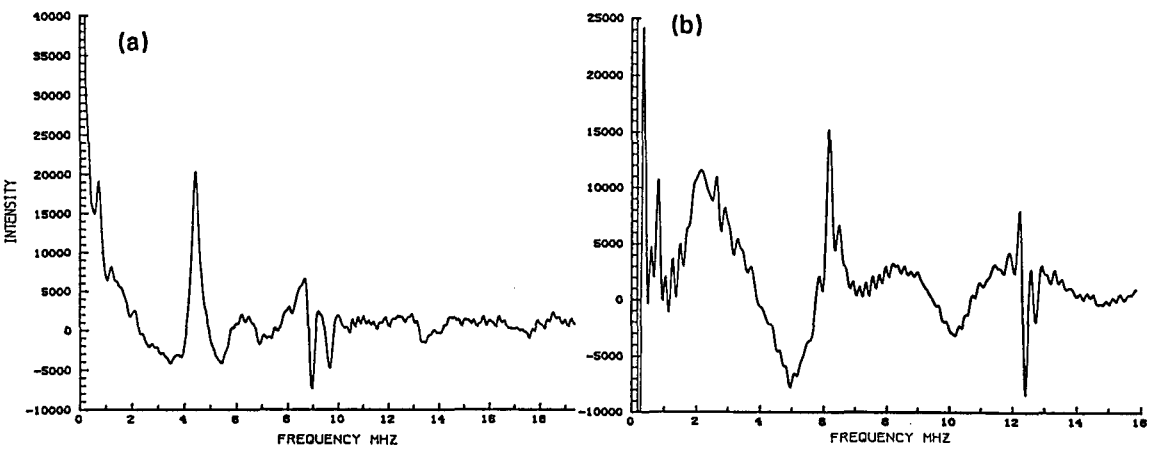

Figure 4. Cosine FT of 2-pulse ESEEM from $Cu(benzac)_2$ - pyridine (1:1) in toluene at 4.01 GHz, 5K. (a) B_o = 1045 Gauss ($g_{parallel}$), (b) B_o = 1450 Gauss ($g_{perpendicular}$).

At S-band, as at X-band, strong orientation selection is evident. Only the spectra taken in the parallel region of the EPR spectrum from samples with equimolar concentrations of $Cu(benzac)_2$ and pyridine yielded spectra with well defined features aside from matrix peaks. A three pulse ESEEM pattern recorded near the low field edge (magnetic field orientations near the Cu-Py line) of the EPR spectrum is shown in Figure 5.

In these patterns, the most prominent features are two peaks centered close to 1 MHz. Simulations with nitrogen hyperfine and quadrupole coupling parameters previously derived from orientation-selected X-band ESEEM data of the same complex in ca. 30% pyridine [20] produced one prominent peak, at ca. 1.0 MHz. Simulations with NANGSEL showed this peak to contain (be sensitive to) the rhombic component (ηe^2qQ) of the nitrogen quadrupole coupling matrix, but not to the axial component or the asymmetry parameter alone, as illustrated in Figure 6.

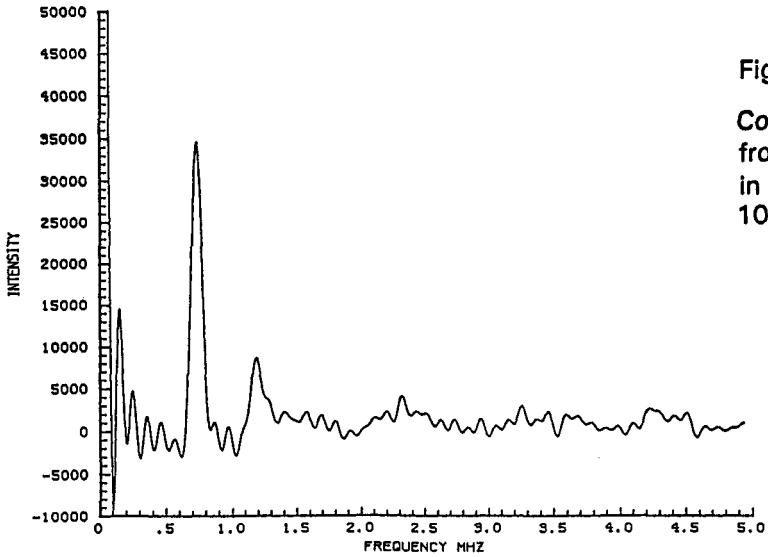

Figure 5.

Cosine FT of 3-pulse ESEEM from Cu(benzac)$_2$-pyridine (1:1) in toluene at 4.01 GHz, 1045 Gauss ($g_{parallel}$), 5K.

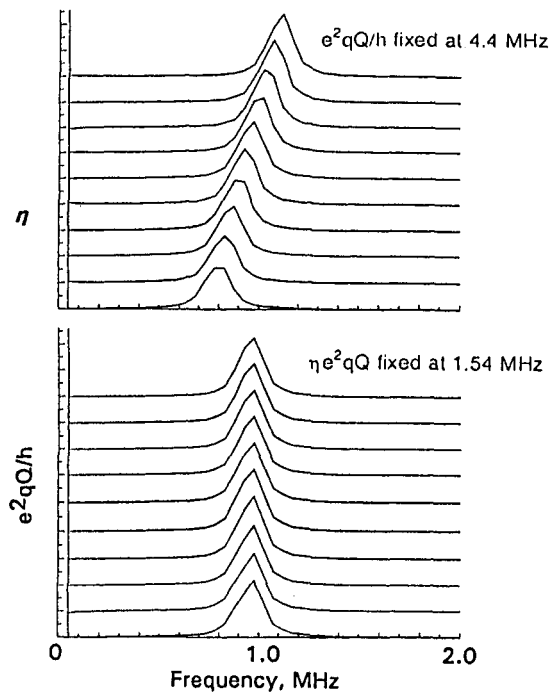

Figure 6.

Simulations of parallel-region S-band ESEEM spectra of the Cu(benzac)$_2$•2Py complex, with parameters as reported in [20], with ηe^2qQ fixed at 1.54 MHz or e^2qQ fixed at 4.4 MHz.
Below:
Starting from bottom, e^2qQ/h = 3.4 MHz and at 0.2 MHz increments.
Above:
Starting from bottom, η = 0.25 and at increments of 0.2

Furthermore, the single peak proves to bifurcate with adjustment of the nitrogen hyperfine coupling parameters (both isotropic and anisotropic). Parameters obtained by fitting the two prominent peaks in the S-band ESEEM spectra of the Cu(benzac)$_2$•Py complex is $g_{x,y,z}$ = 2.067, 2.062, 2.302; $A(Cu)_{x,y,z}$ = 25, 25, 492 MHz; electron-nitrogen distance = 2.4Å; $a(N)_{iso}$ = -0.5 MHz; e^2qQ = 4.4 MHz; η = 0.30. These parameters must be regarded as preliminary; further S-band ESEEM work on both the •Py and •2Py species with both isotopes of nitrogen is underway to confirm our initial interpretation and refine the parameters.

D. *m*-Dinitrobenzene radicals on γ-alumina

For a paramagnetic system of isotropic g-tensor interacting with a nucleus of $I \geq 1$, if the super-hyperfine interaction is also isotropic, the Hamiltonian will include terms that can give modulations,

$$\hat{H}_n = A\mathbf{S}\cdot\mathbf{I} - g_n\beta_n\mathbf{B}_o\cdot\mathbf{I} + \mathbf{I}\cdot\boldsymbol{P}\cdot\mathbf{I} \qquad (2)$$

where A is the isotropic super-hyperfine constant of the nucleus, $\mathbf{B}_o$ the external static

magnetic field vector, **S** and **I** are usual electron and nuclear spin vectors, and ***P*** nuclear quadrupole tensor. The electron spin **S** has two orientations in external magnetic field. Thus Eqn. (2) can be rewritten as

$$\hat{H}_n = \mathbf{U}\cdot\mathbf{I}(\pm A/2 - g_n\beta_n B_o) + \mathbf{I}\cdot\boldsymbol{P}\cdot\mathbf{I} \qquad (3)$$

where **U** is a unit vector along the direction of static magnetic field. The magnitudes (energies) of the two electron spin manifolds will move in opposite directions as the external magnetic field increases. This implies that for quadrupolar nuclei ($I \geq 1$), an external magnetic field of magnitude B_o can be chosen such that the nuclear Zeeman interaction cancels the super-hyperfine interaction in one of the two electron spin states. The ensuing nuclear energy levels, in the electron spin manifold in which the cancellation occurs, correspond to the pure nuclear quadrupole states,

$$\hat{H}_n^{eff} = \mathbf{I}\cdot\boldsymbol{P}\cdot\mathbf{I} \qquad (4)$$

This permits a direct observation of the NQR transitions, the frequencies of which can be used to calculate the quadrupole parameters (e^2qQ and η). Recently Cosgrove and Singel [8,10] have studied this phenomenon in the m-DNB radical generated on γ-alumina, and performed X-band (8-11 GHz) and C-band (4-6 GHz) ESEEM experiments in an attempt to realize "exact cancellation". Their work suggested that the equivalence Zeeman field ($B_o = A_{iso}/2g_n\beta_n$) lies lower than those spanned by their experiments. Utilizing S-band frequencies and fields, we have more nearly achieved experimental realization of the "exact cancellation" condition in this system, and direct observations of nearly pure nitrogen nuclear quadrupole transitions have been made from the Fourier transformed ESEEM spectra. S-band ESEEM also has proved sensitive to the surface effects of γ-alumina on the NQR parameters of the remote nitrogen atom in m-DNB radicals.

Three-pulse ESEEM experiments were performed at four different microwave frequencies from 2 to 4 GHz: 3.85, 3.24, 3.01, and 2.81 GHz. The frequency-domain spectra, obtained by cosine Fourier transformation with zero-filling, are shown in Figure 7. In the 3.85 GHz experiment, both ^{14}N and ^{15}N enriched *meta*-dinitrobenzene samples were studied, in an effort to differentiate the hyperfine and nuclear quadrupole interactions. A thorough static magnetic field (B_o) and τ-effect survey also was done on ^{14}N samples at this excitation frequency: there is no obvious τ-suppression effect observed in three-pulse ESEEM experiments at excitation microwave frequencies under 4 GHz, which suggests that nuclear quadrupole coupling terms dominate the modulation pattern. The X-band cw-EPR spectrum of m-DNB radical adsorbed on γ-alumina spans a field range of ca. 75 gauss, and the ESE signal was observable in the entire field range. The pattern of nuclear frequency modulation does not show any noticeable change in this range although the spin echo intensity may vary

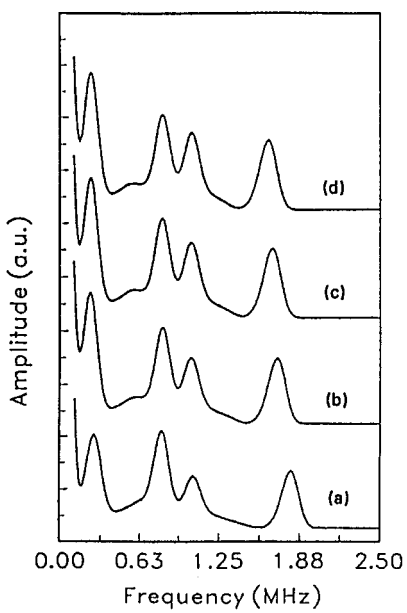

Figure 7.

Cosine FT of ESEEM from *m*-DNB at
(a) 3.85 GHz
(b) 3.24 GHz
(c) 3.01 GHz
(d) 2.81 GHz

depending on where the static magnetic field center is set. A single nitrogen modulation frequency was observed when a ^{15}N sample was used; compared to ^{14}N, the ^{15}N modulation is shallow.

A four-line pattern is observed from ^{14}N-containing samples at all four excitation frequencies. The four peaks are due to remote nitrogen (#2) as identified in reference [10]. At 3.01 GHz, the nuclear modulation frequencies are 0.229, 0.8, 1.029, and 1.653 MHz. At 2.81 and 3.24 GHz, the first three peaks share the same frequency values with the spectrum obtained at 3.01 GHz, while the frequency of the fourth peak changes. We assign the first three peaks as *pure* NQR transitions from one electron spin manifold, ν_0 = 0.229, ν_{-1} = 0.8, and ν_{+1} = 1.029 MHz; and ν' = 1.653 MHz is a nuclear transition from another electron spin manifold.

A comparison of ^{14}N and ^{15}N modulation patterns demonstrates that the hyperfine coupling of the distant nitrogen is very close to isotropic, with a value of A_{iso} between 0.60 and 0.67 MHz for ^{14}N. The relatively large uncertainty in this value is due to the weak and somewhat broad character of the frequency domain peak for ^{15}N. The measurement allows us to predict that for distant ^{14}N in m-DNB, $B_0 = A_{iso}/2g_n\beta_n$ at a value of ca. 980 Gauss, which at g = 2 requires a microwave frequency of 2.7 GHz. Thus, we are almost exactly at the predicted value for "exact cancellation" at the lowest of our microwave frequency measurements. As in S-band studies of DPPH discussed in Section B., the nearly pure NQR frequencies are observed over a range of field values. The NQR parameters thus calculated are given in Table 1.

Table 1. NQR Parameters for m-DNB on γ-alumina

Radical	*Data Analyzed*	A_{iso} *(MHz)*	e^2qQ *(MHz)*	η
Freshly-made	Cosine FT		1.243	0.36
	Time-domain simulation	0.65	1.245	0.36
ca. 1 year	Cosine FT		1.219	0.37
	Time-domain simulation	0.65	1.220	0.37

In his paper on an EPR investigation of m-DNB on γ-alumina, Flockhart et. al.[30] first observed the increase of EPR signal intensity as a function of contact time following the introduction of a m-DNB/benzene solution onto the alumina surface. We observed a similar increase and, moreover, continue to observe it over several days. If we use a more extended time frame of, say, a year, we can also see the three cw-EPR peaks becoming broader. With the help of ESEEM spectroscopy we observe a corresponding change in the modulation frequencies from the remote NO_2 nitrogen atom during the same time period of a year. This change is mainly reflected in a slight alteration of the nuclear quadrupole coupling constants, e^2qQ and η (see Table 1). Among the possible mechanisms that copuld account for this change with time in the NQR parameters, two are: (1) increasing spin density on the distant nitrogen, and (2) a surface structure change. The first mechanism is very unlikely since virtually no change in the magnitude of A_{iso} for the distant nitrogen is observed with time. If there were an increase in the spin density at the remote nitro group, we almost certainly would have observed an increase in A_{iso}. Furthermore, Cheng and Brown [31] measured the NQR parameters for m-DNB radicals in liquid phase. The values they report are: e^2qQ = 1.232 MHz and η=0.36. It is likely that the differences between their NQR parameters and those observed in this study are due primarily to the differences in environment between m-DNB radicals in isotropic solution and adsorbed on an alumina surface, which is known to produce significant electric field gradients on adsorbed radicals [32]. The large magnitude of the shifts in NQR parameters between solution and surface, here attributed to surface effects, would seem to point to modifications of the surface environment of m-DNB radicals with time as a more likely mechanism to account for changes in the NQR parameters. S-band ESEEM from radicals like m-DNB thus seems to hold promise as a very sensitive technique to follow weak surface interactions.

Acknowledgements

Gratitude is expressed to Professor Jeffrey B. Cornelius, Principia College, Elsah, IL, for time-domain simulation software used in several of the studies reported here. Thanks also to Dr. Jack Peisach, Biotechnology Resource in Pulsed EPR Spectroscopy, Albert Einstein College of Medicine, Bronx, NY (RR-02583), for partial support in developing analysis software. This research was supported by the Illinois EPR Research Center, an NIH Biotechnology Resource Center (RR-01811), and through grants from the NIH (to RBC, GM42208), the Illinois Department of Energy and Natural Resources, Coal Development Board, through the CRSC, and the U. S. Department of Energy (to RLB, DEFG 22-88PC8921).

REFERENCES

1. J. P. Gordon and K. D. Bowers, Phys. Rev. Letters, 1, 368 (1958).
2. W. B. Mims, K. Nassau, and J. D. McGee, Phys. Rev., 123, 2059 (1961).
3. J. Schmidt, Chem. Phys. Letters, 14, 411 (1972).
4. P. F. Liao and S. R. Hartmann, Phys. Rev., B8, 69 (1973).
5. H. L. Flanagan and D. J. Singel, Chem. Phys. Letters, 137, 391 (1987).
6. R. T. Weber, J. A. J. M. Disselhorst, L. J. Provo, J. Schmidt, and W. Th. Wenckebach, J. Mag. Reson., 81, 129 (1989).
7. H. L. Flanagan, G. J. Gerfen, A. Lai, and D. J. Singel, J. Chem. Phys., 88, 2162 (1988).
8. S. A. Cosgrove and D. J. Singel, J. Chem. Phys., 94, 2619 (1990).
9. A. Schweiger, Angew. Chem. Int. Ed. Engl., 30, 265 (1991).
10. S. A. Cosgrove and D. J. Singel, J. Phys. Chem., 94, 8393 (1990).
11. A. Lai, H. L. Flanagan, and D. J. Singel, J. Chem. Phys., 89, 7161 (1988).
12. R. L. Belford, R. B. Clarkson, J. B. Cornelius, K. S. Rothenberger, M. J. Nilges, and M. D. Timken, in: *Electronic Magnetic Resonance of the Solid State*, ed. J. A. Weil, Canadian Society for Chemistry, Ottawa, 1987, p. 21.
13. H. C. Crookham, Ph. D. Dissertation, University of Illinois, Urbana, 1990.
14. J. S. Hyde and W. Froncisz, in: *Advanced EPR*, ed. A. J. Hoff, Elsevier, Amsterdam, 1989, pg. 277.
15. S. Pfenniger, J. Forrer, A. Schweiger, and Th. Weiland, Rev. Sci. Instrum., 59, 752 (1988).
16. D. R. Brown, Ph. D. Dissertation, University of Illinois, Urbana, 1990.
17. R. B. Clarkson, R. L. Belford, K. S. Rothenberger, and H. C. Crookham, J. Catal., 106, 500 (1987).
18. P. Hon, C. E. Pfluger, and R. L. Belford, Inorg. Chem., 5, 516 (1966).
19. W. B. Mims, J. Mag. Res., 59, 291 (1984).
20. J. B. Cornelius, J. McCracken, R. B. Clarkson, R. L. Belford, and J. Peisach, J. Phys. Chem., 94, 6977 (1990).
21. K. S. Rothenberger, H. C. Crookham, R. L. Belford, and R. B. Clarkson, J. Catal., 115, 430 (1989).
22. R. B. Clarkson, M. D. Timken, D. R. Brown, H. C. Crookham, and R. L. Belford, Chem. Phys. Letters, 163, 277 (1989).
23. S. A. Dikanov, A. V. Astashkin, and Yu. D. Tsvetkov, J. Struct. Chem., 25, 200 (1984).
24. H. L. Flanagan and D. J. Singel, J. Chem. Phys., 87, 5606 (1987).
25. N. S. Dalal, J. A. Ripmeester, and A. H. Reddoch, J. Mag. Res., 31, 471 (1978).
26. D. J. Singel, private communication.
27. B. Kirste and H. van Willigen, J. Phys. Chem., 87, 781 (1983).
28. T.A. Henderson, G.C. Hurst, R.W. Kreilick, J. Am. Chem. Soc., 107, 7299 (1985).
29. J. B. Cornelius, Ph.D. Dissertation, University of Illinois, Urbana, 1987.
30. B. D. Flockhart, I. R. Leith, and R. C. Pink, Trans. Faraday Soc., 66, 469 (1969).
31. C. P. Chang and T. L. Brown, J. Mag. Reson., 28, 391 (1977).
32. R. B. Clarkson, in: *Magnetic Resonance in Colloid and Interface Science*, Eds. J. P. Fraissard and H. A. Resing, D. Reidel Publishing Co., Dortrecht, 1980, pg. 425.